NUCLEAR DATA AND MEASUREMENTS SERIES

ANL/NDM-55

Thermal Neutron Calibration of a Tritium Extraction Facility Using the $^{6}Li(n,t)^{4}He/^{197}Au(n,g)^{198}Au$ Cross Section Ratio for Standardization

by

M.M. Bretscher and D.L. Smith

August 1980

ARGONNE NATIONAL LABORATORY,
ARGONNE, ILLINOIS 60439, U.S.A.

NUCLEAR DATA AND MEASUREMENTS SERIES

ANL/NDM-55

THERMAL NEUTRON CALIBRATION OF A TRITIUM EXTRACTION FACILITY USING THE $^{6}Li(n,t)^{4}He/^{197}Au(n,\gamma)^{198}Au$ CROSS SECTION RATIO FOR STANDARDIZATION

by

M. M. Bretscher and D. L. Smith

August 1980

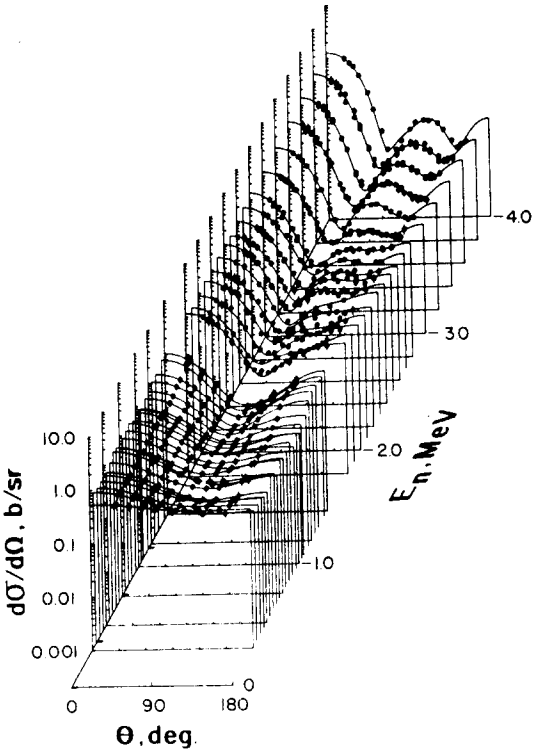

U of C-AUA-USDOE

ARGONNE NATIONAL LABORATORY,
ARGONNE, ILLINOIS 60439, U.S.A.

The facilities of Argonne National Laboratory are owned by the United States Government. Under the terms of a contract (W-31-109-Eng-38) between the U. S. Department of Energy, Argonne Universities Association and The University of Chicago, the University employs the staff and operates the Laboratory in accordance with policies and programs formulated, approved and reviewed by the Association.

MEMBERS OF ARGONNE UNIVERSITIES ASSOCIATION

The University of Arizona
Carnegie-Mellon University
Case Western Reserve University
The University of Chicago
University of Cincinnati
Illinois Institute of Technology
University of Illinois
Indiana University
Iowa State University
The University of Iowa
Kansas State University
The University of Kansas
Loyola University
Marquette University
Michigan State University
The University of Michigan
University of Minnesota
University of Missouri
Northwestern University
University of Notre Dame
The Ohio State University
Ohio University
The Pennsylvania State University
Purdue University
Saint Louis University
Southern Illinois University
The University of Texas at Austin
Washington University
Wayne State University
The University of Wisconsin

ANL/NDM-55

THERMAL NEUTRON CALIBRATION OF A TRITIUM EXTRACTION FACILITY USING THE $^{6}Li(n,t)^{4}He/^{197}Au(n,\gamma)^{198}Au$ CROSS SECTION RATIO FOR STANDARDIZATION

by

M. M. Bretscher and D. L. Smith

August 1980

Applied Physics Division
Argonne National Laboratory
9700 South Cass Avenue
Argonne, Illinois 60439
USA

NUCLEAR DATA AND MEASUREMENTS SERIES

The Nuclear Data and Measurements Series presents results of studies in the field of microscopic nuclear data. The primary objective is the dissemination of information in the comprehensive form required for nuclear technology applications. This Series is devoted to: a) measured microscopic nuclear parameters, b) experimental techniques and facilities employed in measurements, c) the analysis, correlation and interpretation of nuclear data, and d) the evaluation of nuclear data. Contributions to this Series are reviewed to assure technical competence and, unless otherwise stated, the contents can be formally referenced. This Series does not supplant formal journal publication but it does provide the more extensive information required for technological applications (e.g., tabulated numerical data) in a timely manner.

OTHER ISSUES IN THE ANL/NDM SERIES ARE:

ANL/NDM-1 Cobalt Fast Neutron Cross Sections-Measurement and Evaluation by P. T. Guenther, P. A. Moldauer, A. B. Smith, D. L. Smith and J. F. Whalen, July 1973.

ANL/NDM-2 Prompt Air-Scattering Corrections for a Fast-Neutron Fission Detector: $E_n \leq 5$ MeV by Donald L. Smith, September 1973.

ANL/NDM-3 Neutron Scattering from Titanium; Compound and Direct Effects by E. Barnard, J. deVilliers, P. Moldauer, D. Reitmann, A. Smith and J. Whalen, October 1973.

ANL/NDM-4 ^{90}Zr and ^{92}Zr; Neutron Total and Scattering Cross Sections by P. Guenther, A. Smith and J. Whalen, July 1974.

ANL/NDM-5 Delayed Neutron Data - Review and Evaluation by Samson A. Cox, April 1974.

ANL/NDM-6 Evaluated Neutronic Cross Section File for Niobium by R. Howerton, Lawrence Livermore Laboratory and A. Smith, P. Guenther and J. Whalen, Argonne National Laboratory, May 1974.

ANL/NDM-7 Neutron Total and Scattering Cross Sections of Some Even Isotopes of Molybdenum and the Optical Model by A. B. Smith, P. T. Guenther and J. F. Whalen, June 1974.

ANL/NDM-8 Fast Neutron Capture and Activation Cross Sections of Niobium Isotopes by W. P. Poenitz, May 1974.

ANL/NDM-9 Method of Neutron Activation Cross Section Measurement for E_n = 5.5-10 MeV Using the D(d,n)He-3 Reaction as a Neutron Source by D. L. Smith and J. W. Meadows, August 1974.

ANL/NDM-10 Cross Sections for (n,p) Reactions on ^{27}Al, $^{46,47,48}Ti$, $^{54,56}Fe$, ^{58}Ni, ^{59}Co and ^{64}Zn from Near Threshold to 10 MeV by Donald L. Smith and James W. Meadows, January 1975.

ANL/NDM-11 Measured and Evaluated Fast Neutron Cross Sections of Elemental Nickel by P. Guenther, A. Smith, D. Smith and J. Whalen, Argonne National Laboratory and R. Howerton, Lawrence Livermore Laboratory, July 1975.

ANL/NDM-12 A Spectrometer for the Investigation of Gamma Radiation Produced by Neutron-Induced Reactions by Donald L. Smith, April 1975.

ANL/NDM-13 Response of Several Threshold Reactions in Reference Fission Neutron Fields by Donald L. Smith and James W. Meadows, June 1975.

ANL/NDM-14 Cross Sections for the $^{66}Zn(n,p)^{66}Cu$, $^{113}In(n,n')^{113m}In$ and $^{115}In(n,n')^{115m}In$ Reactions from Near Threshold to 10 MeV by Donald L. Smith and James W. Meadows, July 1975.

ANL/NDM-15 Radiative Capture of Fast Neutrons in ^{165}Ho and ^{181}Ta by W. P. Poenitz, June 1975.

ANL/NDM-16 Fast Neutron Excitation of the Ground-State Rotational Band of ^{238}U by P. Guenther, D. Havel and A. Smith, September 1975.

ANL/NDM-17 Sample-Size Effects in Fast-Neutron Gamma-Ray Production Measurements: Solid-Cylinder Samples by Donald L. Smith, September 1975.

ANL/NDM-18 The Delayed Neutron Yield of ^{238}U and ^{241}Pu by J. W. Meadows January 1976.

ANL/NDM-19 A Remark on the Prompt-Fission-Neutron Spectrum of ^{252}Cf by P. Guenther, D. Havel, R. Sjoblom and A. Smith, March 1976.

ANL/NDM-20 Fast-Neutron-Gamma-Ray Production from Elemental Iron: $E_n \lesssim$ 2 MeV by Donald L. Smith, May 1976.

ANL/NDM-21 Note on the Experimental Determination of the Relative Fast-Neutron Sensitivity of a Hydrogenous Scintillator by A. Smith, P. Guenther and R. Sjoblom, June 1976.

ANL/NDM-22 Note on Neutron Scattering and the Optical Model Near A=208 by P. Guenther, D. Havel and A. Smith, September 1976.

ANL/NDM-23 Remarks Concerning the Accurate Measurement of Differential Cross Sections for Threshold Reactions Used in Fast-Neutron Dosimetry for Fission Reactors by Donald L. Smith, December 1976.

ANL/NDM-24 Fast Neutron Cross Sections of Vanadium and an Evaluated Neutronic File by P. Guenther, D. Havel, R. Howerton, F. Mann, D. Smith, A. Smith and J. Whalen, May 1977.

ANL/NDM-25 Determination of the Energy Scale for Neutron Cross Section Measurements Employing a Monoenergetic Accelerator by J. W. Meadows, January 1977.

ANL/NDM-26 Evaluation of the IN-115(N,N')IN-115M Reaction for the ENDF/B-V Dosimetry File by Donald L. Smith, December 1976.

ANL/NDM-27 Evaluated (n,p) Cross Sections of ^{46}Ti, ^{47}Ti and ^{48}Ti by C. Philis and O. Bersillon, Bruyeres-le-Chatel, France and D. Smith and A. Smith, Argonne National Laboratory, January 1977.

ANL/NDM-28 Titanium-II: An Evaluated Nuclear Data File by C. Philis, Centre d'Etudes de Bruyéres-le-Châtel, R. Howerton, Lawrence Livermore Laboratory and A. B. Smith, Argonne National Laboratory, June 1977.

ANL/NDM-29 Note on the 250 keV Resonance in the Total Neutron Cross Section of ^{6}Li by A. B. Smith, P. Guenther, D. Havel and J. F. Whalen, June 1977.

ANL/NDM-30 Analysis of the Sensitivity of Spectrum-Average Cross Sections to Individual Characteristics of Differential Excitation Functions by Donald L. Smith, March 1977.

ANL/NDM-31 Titanium-I: Fast Neutron Cross Section Measurements by P. Guenther, D. Havel, A. Smith and J. Whalen, May 1977.

ANL/NDM-32 Evaluated Fast Neutron Cross Section of Urnaium-238 by W. Poenitz, E. Pennington, and A. B. Smith, Argonne National Laboratory and R. Howerton, Lawrence Livermore Laboratory, October 1977.

ANL/NDM-33 Comments on the Energy-Averaged Total Neutron Cross Sections of Structural Materials by A. B. Smith and J. F. Whalen, June 1977.

ANL/NDM-34 Graphical Representation of Neutron Differential Cross Section Data for Reactor Dosimetry Applications by Donald L. Smith, June 1977.

ANL/NDM-35 Evaluated Nuclear Data File of Th-232 by J. Meadows, W. Poenitz, A. Smith, D. Smith and J. Whalen, Argonne National Laboratory and R. Howerton, Lawrence Livermore Laboratory, February 1978.

ANL/NDM-36 Absolute Measurements of the $^{233}U(n,f)$ Cross Section Between 0.13 and 8.0 MeV by W. P. Poenitz, April 1978.

ANL/NDM-37 Neutron Inelastic Scattering Studies for Lead-204 by D. L. Smith and J. W. Meadows, December 1977.

ANL/NDM-38 The Alpha and Spontaneous Fission Half-Lives of ^{242}Pu by J. W. Meadows, December 1977.

ANL/NDM-39 The Fission Cross Section of ^{239}Pu Relative to ^{235}U from 0.1 to 10 MeV by J. W. Meadows, March 1978.

ANL/NDM-40 Statistical Theory of Neutron Nuclear Reactions by P. A. Moldauer, February 1978.

ANL/NDM-41 Energy-Averaged Neutron Cross Sections of Fast-Reactor Structural Materials by A. Smith, R. McKnight and D. Smith, February 1978.

ANL/NDM-42 Fast Neutron Radiative Capture Cross Section of ^{232}Th by W. P. Poenitz and D. L. Smith, March 1978.

ANL/NDM-43 Neutron Scattering from ^{12}C in the Few-MeV Region by A. Smith, R. Holt and J. Whalen, September 1978.

ANL/NDM-44 The Interaction of Fast Neutrons with ^{60}Ni by A. Smith, P. Guenther, D. Smith and J. Whalen, January 1979.

ANL/NDM-45 Evaluation of $^{235}U(n,f)$ between 100 KeV and 20 MeV by W. P. Poenitz, July 1979.

ANL/NDM-46 Fast-Neutron Total and Scattering Cross Sections of ^{107}Ag in the MeV Region by A. Smith, P. Guenther, G. Winkler and J. Whalen, January 1979.

ANL/NDM-47 Scattering of MeV Neutrons from Elemental Iron by A. Smith and P. Guenther, March 1979.

ANL/NDM-48 ^{235}U Fission Mass and Counting Comparison and Standardization by W. P. Poenitz, J. W. Meadows and R. J. Armani, May 1979.

ANL/NDM-49 Some Comments on Resolution and the Analysis and Interpretation of Experimental Results from Differential Neutron Measurements by Donald L. Smith, November 1979.

ANL/NDM-50 Prompt-Fission-Neutron Spectra of ^{233}U, ^{235}U, ^{239}Pu and ^{240}Pu Relative to that of ^{252}Cf by A. Smith, P. Guenther, G. Winkler and R. McKnight, September 1979.

ANL/NDM-51 Measured and Evaluated Neutron Cross Sections of Elemental Bismuth by A. Smith, P. Guenther, D. Smith and J. Whalen, April 1980.

ANL/NDM-52 Neutron Total and Scattering Cross Sections of ^{6}Li in the Few MeV Region by P. Guenther, A. Smith and J. Whalen, February 1980.

ANL/NDM-53 Neutron Source Investigations in Support of the Cross Section at the Argonne Fast-Neutron Generator by James W. Meadows and Donald L. Smith, May 1980.

ANL/NDM-54 The Nonelastic-Scattering Cross Sections of Elemental Nickel by A. B. Smith, P. T. Guenther and J. F. Whalen, June 1980.

TABLE OF CONTENTS

LIST OF FIGURES

LIST OF TABLES

THERMAL NEUTRON CALIBRATION OF A TRITIUM EXTRACTION FACILITY USING THE $^{6}Li(n,t)^{4}He/^{197}Au(n,\gamma)^{198}Au$ CROSS SECTION RATIO FOR STANDARDIZATION

by

M. M. Bretscher and D. L. Smith

Argonne National Laboratory

ABSTRACT

Absolute tritium activities in neutron-activated metallic lithium samples have been measured by liquid scintillation methods to provide data needed for the determination of capture-to-fission ratios in fast breeder reactor spectra and for recent measurements of the $^{7}Li(n,n't)^{4}He$ cross section. The tritium extraction facility used for all these experiments has now been calibrated by measuring the $^{6}Li(n,t)^{4}He/^{197}Au(n,\gamma)^{198}Au$ activity ratio for thermal neutrons and comparing the result with the well-known cross sections. The calculated-to-measured activity ratio was found to be 1.033 ± 0.018.

I. INTRODUCTION

Years ago a technique[1] was developed for measuring absolute tritium activities induced in metallic lithium samples (usually enriched in ^{6}Li) which had been irradiated in Argonne's fast critical assemblies. From these activities ^{6}Li neutron absorption rates were obtained which, when combined with other data, allowed the determination of capture-to-fission ratios for most of the fissile isotopes in typical fast breeder reactor spectra[2-5]. Absolute ^{6}Li absorption rates determined by this method also permitted the evaluation of the perturbation denominator[6] and the breeding ratio[7] in LMFBR critical assemblies. Finally, the tritium extraction facility developed for these studies has now been used in a recent measurement of the $^{7}Li(n,n't)^{4}He$ cross section in the 7-9 Mev energy range[8].

However, questions have arisen regarding a possible large systematic error associated with the tritium extraction process as a result of a joint study with Dr. H. Farrar of Rockwell International. The Bretscher/Farrar experiment is described in some detail in the Appendix. Briefly, however, it consisted of irradiating, under identical conditions, 16 small aluminum-clad natural lithium samples ($\approx$22 mg) in the form of short thin wires in the thermal column of the Argonne Thermal Source Reactor (ATSR). Because of the $^{6}Li(n,t)^{4}He$ reaction, equal amounts of tritium and helium were produced in each of the samples. Half of the samples were analyzed for helium content by H. Farrar who used a mass spectrometer to measure the $^{3}He/^{4}He$ ratio after the sample had been vaporized in a known quantity of ^{3}He. The remaining samples were analyzed by Bretscher for tritium using the extraction apparatus and methods previously developed for ZPR measurements. Although the precision was good in both sets of measurements, it was found that the measured helium yield

per gram of lithium was about 9% larger than the measured tritium yield. Subsequent measurements by both Farrar and Bretscher have failed to remove this systematic difference. (See Appendix)

Because of the important implications this discrepancy may have on the previous ZPR measurements and on the recent $^{7}Li(n,n't)^{4}He$ cross section determinations, this thermal calibration was undertaken to see if a systematic loss of tritium associated with the extraction procedures could be identified and, if necessary, accounted for. The calibration method consists of simultaneously irradiating in equal thermal fluxes thin gold and lithium foils of the same diameter and equal thicknesses, as measured in units of absorption mean free paths. The measured $^{6}Li(n,\alpha)/^{198}A(n,\gamma)$ activity ratio is then compared with that calculated from the well-known thermal cross sections. Flux perturbation and neutron self-shielding effects cancel in the activity ratio determination provided the foil geometries meet the above conditions and neutron scattering effects within the foils are negligble. The results of this thermal calibration are described below.

II. EXPERIMENTAL METHODS

A. Foil Preparation

To minimize self-shielding corrections, it is necessary to use thin lithium and gold foils for the thermal irradiation. At the same time foils need to be thick enough so that they can be easily handled and weighed with a neglegible mass uncertainty.

With these limitations in mind, lithium metal depleted in ^{6}Li was obtained from the Stable Isotopes Division of the Oak Ridge National Laboratory. This material contained about 1.5 wt% ^{6}Li. Because of the importance of knowing the

^{6}Li content in the lithium samples as accurately as possible, additional mass spectrum measurements were made at both Oak Ridge and Argonne. The results of these measurements are discussed in the following section.

Since lithium is an extremely reactive metal, foil samples were prepared in a clean dry argon atmosphere. A special glove box with thick rigid walls was first evacuated to remove N_2, O_2 and water vapor, all of which react quickly with lithium metal, and then filled to one atmosphere with 99.999% pure argon (supplier's specification). Within this atmosphere the lithium metal billet was removed from its shipping container, cleaned of excess mineral oil by blotting with paper towels, placed in a new stainless steel beaker and melted. After scraping off surface scum, the molten metal was poured into a stainless steel extrusion die and allowed to cool. Upon reaching ambient temperature, the lithium metal was extruded through a 1.125 in. × 0.008 in. slit using a hydraulic jack. Foil samples, 0.750 in. diameter, were punched from the central portion of this ribbon and weighed on a microbalance. Each foil was weighed three times and the balance was frequently calibrated with a standard 50 mg mass. Throughout these operations the lithium foils retained their bright shiny appearance. Following the weighing operation the foils were placed into specially prepared aluminum (Type 1100) covers, 0.018 in. thick, designed to accurately center the sample. These assemblies were put into individual dessicators, removed from the glove box, and sealed around the circumference by a cold welding technique using a hydraulic press. Except for the final sealing operation, which required less than 30 sec. per sample, all operations were performed in the argon-filled glove box. Figure 1 shows a photograph of the various stages of the lithium foil fabrication.

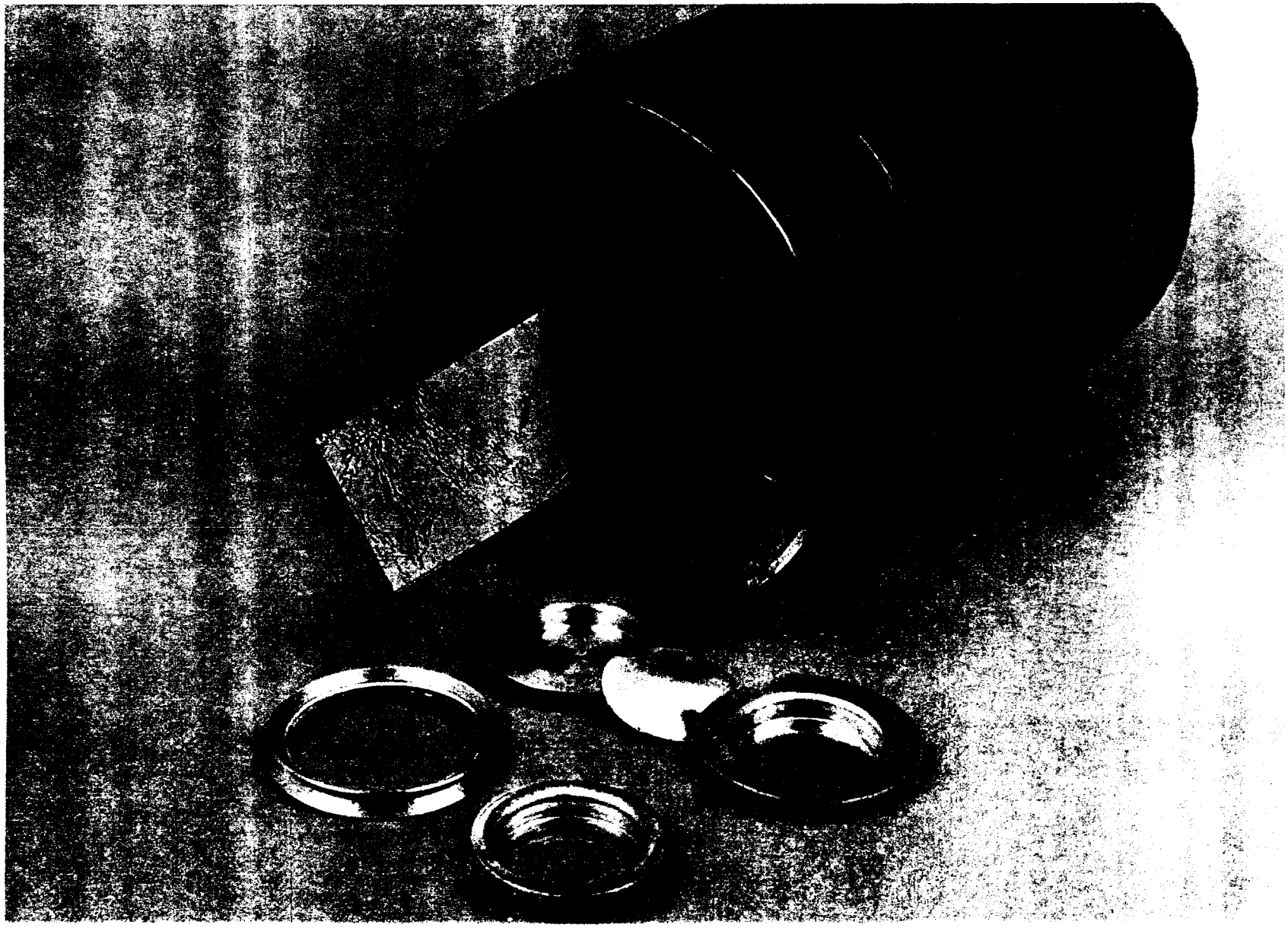

Fig. 1. Miscellaneous Parts for Lithium Foil Assembly - Extrusion die (.008" x 1-1/8" slit), aluminum covers, punched foil, sealed lithium foil assemlby, and aluminum flashing.

Following assembly, the sealed samples were placed in a chamber and subjected to ~ 2 atm of helium pressure for an hour. They were then checked for leaks using a helium mass spectrometer leak detector. The total assembly mass of each sample was also determined shortly after the sealing operation. Since these initial leak test operations were performed about 4 months before the samples were used, they were repeated immediately before the irradiation. None of the samples used in the thermal calibration measurements gave any evidence of leaking by these tests, providing assurance that no tritium was lost in the interval between neutron irradiation and tritium extraction. However, one sample, foil #5, showed an apparent mass increase, suggesting a leak and subsequent reaction with air, and so was rejected. Table I summarizes the foil and assembly masses.

Three fourths inch diameter gold foils where punched from a sheet of gold 0.0005 in. thick and having a purity of 99.999% as specified by the supplier. Aluminum covers, identical to those used for the lithium foils, were used to enclose the gold foils during the irradiation. Gold foil masses are also included in Table I.

B. Lithium Sample Assay

The lithium assay provided by the Isotopes Division of the Oak Ridge National Laboratory at the time the sample was purchased is reproduced in Table II. Unfortunately, no estimate of the error associated with these measurements was given, nor could the original mass spectra data be traced since these records had been destroyed. Because of the importance of knowing the ^{6}Li content of the foils to the best possible accuracy, additional mass spectrum measurements were made at both ANL and ORNL. These results are shown in Table III.

Table I. Lithium and Gold Foil Masses

Li Foil	Mass[a] g	Assembly Mass,[b] g Initial	Final	Au Foil	Mass[a] g
1	0.033136	1.32970	1.32964	1	0.069120
2	0.033615	1.34251	1.34249	2	0.069865
				3	0.070850
4	0.032855	1.34044	1.34036	4	0.070050
5[c]	0.031730	1.33430	1.33829	5	0.070325
6	0.031135	1.33424	1.33422	6	0.067690
				7	0.069885
				8	0.069920
9	0.030380	1.32882	1.32871	9	0.070385
10	0.030192	1.33502	1.33491	10	0.070690
				11	0.068040
				12	0.069395
13	0.032990	1.32950	1.32945	13	0.067060
14	0.033266	1.33547	1.33540	14	0.070940
				15	0.070335
16	0.033240	1.32975	1.32961	16	0.070440
17	0.033420	1.32280	1.32276	17	0.070075
30	0.033185	1.32985	1.32976	18	0.068620
				19	0.070780
				20	0.070460
				21	0.069455
				22	0.069602
				23	0.070280

[a]The uncertainty in the foil mass is ± 0.01 mg.
[b]The uncertainty in the assembly mass is ± 0.08 mg.
[c]Sample rejected because increase in assembly mass suggests leak.

Table II. Lithium Sample Assay (ORNL Isotope Sales)

Batch No.	4726340
Atom % ^{7}Li	98.22
Wt % ^{7}Li	98.47
% Li	99.8500
% C	0.0744
% Cl	0.0015
% Heavy Metals	0.0083
% N	0.0107

Metal	PPM
Ag	< 1
Al	< 10
Ba	< 10
Ca	125
Cd	< 6
Co	< 20
Cr	< 1
Cu	10
Fe	< 20
K	< 20
Mg	100
Mn	< 1
Mo	< 4
Na	< 60
Nb	< 20
Ni	< 10
Pb	< 4
Si	< 25
Sn	< 20
Sr	10
V	< 10
W	< 100

Table III. Mass Spectroscopic Measurements of Lithium Foil Material (ORNL Batch No. 4726340)

Laboratory	$^{7}Li/^{6}Li$ Ratio	Atom % ^{6}Li	Weight % ^{6}Li	Weight % Li
ORNL-Isotope Sales	55.18±0.63[a]	1.78±0.02[a]	1.530±0.017[a]	99.85
ANL[b]	54.04±0.27	1.8169±0.0089	1.5617±0.0077	99.15±0.37
ORNL-J. R. Walton	54.423±0.058	1.8043±0.0018	1.5509±0.0016	
Weighted Ave.:			1.5512±0.0020	

[a]Error estimate only. Based on conversation with J. A. Carter and J. Franklin of ORNL.

[b]Measurements made by E. L. Callis, A. E. Essling, G. Reedy, R. J. Meyer and K. J. Jensen of ANL.

The exceptional accuracy of the last ORNL measurement resulted from the use of a primary standard whose ^{6}Li content was very well known (i.e. 2.308 ± 0.0001 atom % ^{6}Li). The error quoted in Table III for this measurement is the result of combining the uncertainty of the standard with the random error associated with the determination of the ^{7}Li-to-^{6}Li atom ratio for both the standard and the sample.

In addition to the mass spectrum measurement, the total Li content of the foil material was measured at ANL by isotopic dilution methods. Four unirradiated lithium foil samples were used for these measurements. After cutting off the seal, the aluminum top was removed and the exposed lithium foil dissolved in a known amount of alcohol. A known spike of ^{6}Li was added and the lithium mass spectrum of the resulting solution determined. Since the mass spectrum of the foil material had been measured previously, the total lithium content of the foil could be evaluated. Because traces of lithium had not dissolved in the alcohol, the aluminum clad material for each sample was dissolved in HCl and the residual lithium determined by atomic absorption methods. Results of these isotopic dilution/atomic absorption measurements are also shown in Table III.

C. ATSR Irradiations

Lithium and gold foils were simultaneously activiated in the graphite thermal column of the Argonne Thermal Source Reactor (ATSR). The foil assemblies were mounted on an aluminum disk 10 inches in diameter and 1/16 inch thick, in twelve equally spaced 13/16 inch diameter holes located at a radial distance of 4.25 inches from center of the disk. During the irradiations the disk was rotated at a uniform speed by means of an electric motor such that all the foils were equally irradiated. The disk was located in a void having a 4×13

inch cross section. During irradiations the plane of the disk was parallel to the reactor leakage face and about 100 cm from it, with the disk axis aligned with the center line of the graphite thermal column. The various foil irradiations are described in Table IV.

Table IV. ATSR Foil Irradiations

Date	Reactor Power, kW	Time at Power, min.	Purpose
4/10/80	5	15	Activation of aluminum clad lithium and gold foils.
4/11/80	5	15	Activation of gold foils for cadmium ratio measurements.
4/17/80	10	15	Activation of some lithium foils and additional gold cadmium ratio measurements.
5/28/80	0.1	7.5	Gold foil activations to determine gamma effeciency of Ge(Li) detector by $4\pi\beta$-γ coincidence counting.

NOTE: Cadmium covers for the cadmium ratio measurements had a thickness of 0.041 in.

D. Tritium Extraction Procedures

The process for removing tritium from activated lithium samples has been described previously[1], but in the interest of completeness will be summarized here. Tritium is removed from irradiated lithium samples by an isotopic dilution method[9] using normal hydrogen as the carrier gas. The extraction apparatus is illustrated in Fig. 2. After placing the irradiated sample in the furnace, the system is evacuated and valved off, and about 1 atm of ultra-pure (99.999%) hydrogen is added from the calibrated reservoir. As the oven temperature increases, the sample melts and molten LiH forms at about 750°C. Additional hydrogen is added to maintain a pressure of ~ 1 atm as the temperature continues to rise.

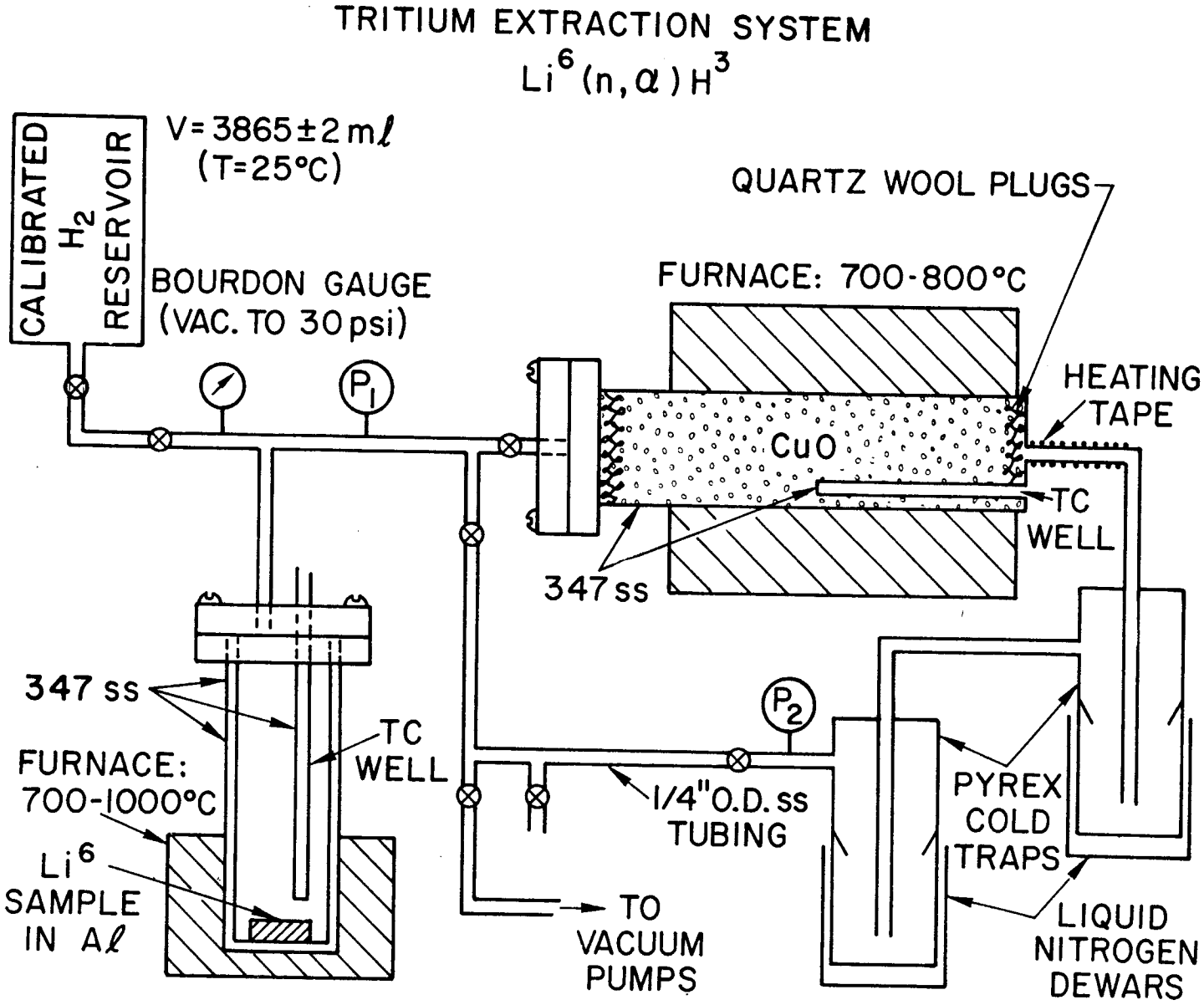

Fig. 2. Tritium Extraction System for Irradiated Lithium Samples

As the temperature in the lithium oven approaches 900°C, lithium hydride readily decomposes with the liberation of a mixture of hydrogen and tritium gas. Using a metering valve, this hydrogen-tritium mixture is then allowed to slowly pass over a hot (~ 750°C) bed of freshly activated CuO. The hydrogen reduces the CuO with the formation of water vapor which is collected in liquid nitrogen cold traps, carefully weighed and sealed in glass ampules for subsequent analysis by liquid scintillation counting methods. The run is terminated when all the hydrogen in the calibrated reservoir has been converted to water, which is then vacuum distilled into the second trap and carefully weighed. In a typical run about 5.8 grams of tritiated water are collected.

To prevent the possibility of cross contamination, a fresh stainless steel (Type 347) liner is used for each sample analysis. Before use, these liners are treated with 6 molar HCl, cleaned, and then outgassed for 6 hours in a vacuum oven at 1000°C. Type 347 stainless steel was chosen for the liners and furnace walls because of its low hydrogen permeation rates[10] and because it is more corrosion-resistant to molten lithium and lithium hydride than most materials.

A greater fraction of hydrogen is converted to water if freshly activated CuO is used in place of a commercial grade. This material is prepared by passing hydrogen over commercial grade CuO (in wire form) at a temperature of about 350°C until all the CuO has been reduced to copper. After pumping out the excess hydrogen, the oven temperature is raised to about 500°C and oxygen is allowed to pass over the bed until a freshly activated surface of CuO forms. The CuO oven is then outgassed for about 15 hours at 750°C before beginning the extraction process.

The initial pressure in the calibrated H_2 reservoir is accurately measured by means of a fused quartz pressure gauge, manufactured by Texas Instruments Company and calibrated against NBS standard weights. Periodically, this gauge calibration is verified at atmospheric pressure by comparing the reading with that obtained from an absolute mercury barometer. A typical set of such measurements is shown in Table V. The volume of the hydrogen reservoir was initially calibrated by carefully weighing the amount of distilled water required to fill the tank. Later, a second calibration was performed in which a special gas cylinder was fabricated whose volume was accurately determined from the known internal dimensions. By measuring the initial and final pressures when hydrogen gas was isothermally expanded from one cylinder to the other, the volume of the hydrogen reservoir was obtained. Combining the results of both calibrations gave the volume $V = 3870 \pm 4$ ml.

Knowing the initial values of P, V, T for the hydrogen carrier gas and the final mass of water collected, it was found that in a typical run about 0.8% of hydrogen was lost during the extraction process. Without a lithium sample present this observed loss amounted to about 0.3% with the lithium oven on and about 0.1% with the oven off.

Most of the hydrogen loss during the extraction results from the condensation of LiH onto the cooler surfaces of the liner near the top of the oven. Some hydrogen is also lost by adsorption and permeation into the furnace walls. However, a correction for these losses can be applied by the methods described above if one assumes that the fractional tritium loss is the same as that for hydrogen.

This last assumption was tested in the Bretscher/Farrar measurements described in the Appendix. These irradiated samples had a high-enough

activity so that, in principle, a 1% tritium loss in the Li-Al residue could be measured. For some of these samples a second tank of hydrogen was used following the primary extraction. Then without opening the system to air and with the lithium oven cooled to room temperature, the lithium-aluminum residue was dissolved in water and the released hydrogen converted to steam and collected in the cold traps. The insoluble aluminum residue was removed from the water sample by centrifuge techniques and the dissolved lithium by triple vacuum distillation. Tritium loss during the primary extraction was then determined from the activity of these water samples. The results are shown in Table VI. It is seen that tritium loss is adequately accounted for by the measured hydrogen loss during the primary extraction. Each of these natural lithium samples had a mass of about 23 mg. If all the lithium in the residue consisted of LiH, the expected hydrogen loss would be about 0.5%. Adding this to the measured 0.2% loss by adsorption and permeation gives a total hydrogen loss of about 0.7%. This is consistent with the observed loss shown in Table VI.

E. Tritium Activity Measurement

The activity of the tritiated water samples was determined by liquid scintillation counting. Each sample was diluted with an accurately weighed amount (~ 5 ml) of laboratory distilled water, divided in two, and counted in two different facilities. Both counting facilities were calibrated by substandards prepared from the NBS tritiated water standard SRM 4926-C[11] whose stated activity was 3.406×10^3 dps/g (± 0.63%) on the reference date 9/3/78. The tritium activity of Argonne's distilled water was recently measured[12] to be 3.02 dpm/g (± 2%) and so for the purposes of these measurements introduces a negligible correction. For decay corrections a tritium half life of 12.33 ± 0.04 yr[13] was assumed using Sher's[14] error estimate.

Table V. Calibration at Atmospheric Pressure Fused Quartz Gauge vs. Barometer

Date	Fused Quartz Gauge psia	Mercury Barometer psia
9/24/79	14.410 ± 0.002	14.409 ± 0.004
9/25/79	14.435 ± 0.002	14.430 ± 0.004
9/26/79	14.460 ± 0.002	14.456 ± 0.004
9/27/79	14.379 ± 0.002	14.381 ± 0.004
9/28/79	14.290 ± 0.002	14.301 ± 0.004
4/15/80	14.129 ± 0.002	14.148 ± 0.004
4/16/80	14.466 ± 0.002	14.471 ± 0.004
4/17/80	14.459 ± 0.002	14.465 ± 0.004
6/3/80	14.333 ± 0.002	14.347 ± 0.004
6/4/80	14.463 ± 0.002	14.461 ± 0.004

Table VI. Expected and Observed Tritium Losses During Extraction Process

Sample	Irradiation Date	$\frac{m(C)^a}{m(E)}$	$\frac{A+A_r{}^b}{A}$
M 4	1/21/77	1.0073	1.0053
M 8	1/21/77	1.0068	1.0041
M 12	1/21/77	1.0075	1.0051
M 16	1/21/77	1.0065	1.0077
M 20	1/21/77	1.0074	1.0067
M 22	1/21/77	1.0091	1.0041
M 30	1/21/77	1.0080	1.0080
M 22	7/1/77	1.0070	1.0060
M 24	7/1/77	1.0077	1.0054

[a] $m(C) \equiv$ calculated water mass from initial P, V, T hydrogen measurements.
$m(E) \equiv$ measured mass of collected water for primary extraction.

[b] $A \equiv$ measured activity of primary water sample.
$A_r \equiv$ measured activity following primary extraction, mostly associated with Li-Al residue.

One of the liquid scintillation counting facilites is a non-commercial instrument[15] used by ANL's Applied Physics Division. This instrument uses two RCA 8850 photomultiplier tubes facing each other in a silicone oil-filled plenum and operated at room temperature. The electronic analysis of coincidence pulses is similar to that described in Ref. 16 except no anticoincidence shield is provided for reducing background counts. Precision cylindrical vials with flat quartz windows 1.500 inches in diameter and having a volume of 12.0 ml are fitted between the two tubes. To determine the tritium activity, 5 ml of the water sample is dissolved in 25 ml of a dioxane-base liquid scintillator[17]. This solution is first bubbled with pure argon to inhibit quenching effects of dissolved oxygen and then pipetted into two counting vials. The efficiency of the counting system, as determined with the NBS standard, is typically about 40% for the dynode channels and 43% for the anode channels, with corresponding background count rates of 0.6 and 1.3 cps, respectively.

Samples were also counted on a commercial liquid scintillation counting facility[18] with automatic sample changing features by D. L. Bowers of the Chemical Engineering Division. With this instrument and Packard's[18] scintillation cocktail INSTA-GEL, 43% counting efficiencies are typical with background count rates of 15-20 cpm. The low background count rates are mostly the result of the phototubes operating in a refrigerated environment (13°C).

Within counting statistics, the same specific activities were measured with each counting facility.

F. Gold Activity Measurement

The disintegration rate of ^{198}Au in thermal neutron activated foils was measured with a Ge(Li) detector which was calibrated by two independent

methods. To correct for decay, a ^{198}Au half life of 2.697 ± 0.003 d[13] was assumed.

The first calibration method involved the irradiation of several 0.750 inch diameter 1/2-mil thick gold foils mounted on the rotating disk in the ATSR graphite thermal column. For each foil the absolute activity was determined by $4\pi\beta$-γ coincidence counting. Various corrections were applied to the data as discussed in Ref. 19. These calibrated foils were then counted in a close, but reproducible, geometry using the Ge(Li) detector adjusted to accept the 412-keV gamma rays from ^{198}Au decay. These measurements provide an efficiency calibration for the Ge(Li) detector which does not require the use of any standards, nor an accurate knowledge of the gamma-ray decay branching factor for ^{198}Au. The results of this calibration are summarized in Table VII. It is seen that the efficiency of the Ge(Li) detector for measuring ^{198}Au disintegrations was 0.01934 (±0.53%) when the full-energy peak yield of the 412-keV gamma rays was recorded in a close, reproducible geometry.

The second approach for calibrating the detector required the use of standard gamma ray sources and a knowledge of the gamma-ray branching ratio for the decay of ^{198}Au. Two standard gamma-ray sources were used. Each was a sealed point source mounted on mylar. These sources were obtained from different suppliers, and they had been independently calibrated. A ^{137}Cs source was obtained from the U.S. National Bureau of Standards.[20] The quoted accuracy in the yield of 661-keV gamma rays is ±2.2%. A ^{152}Eu source was obtained from the Laboratoire de Metrologic des Rayounemeuts Ionisants, Saclay, France.[21] This source produces several gamma-rays. The quoted uncertainties ranged from ± 2.0% for the strongest transition to ± 6.1% for the weakest transition.

Table VII. Calibration of Ge(Li) Detector for 412 KeV Gamma Rays Using a $4\pi\beta$-γ Counter

Au Foil	Mass, g	dps/g ($4\pi\beta$-γ)	cps/g Ge(Li)	Efficiency %
2	0.069865	20973	406.71	1.9392
4	0.070050	20915	404.35	1.9333
5	0.070325	20944	404.06	1.9292
7	0.069885	20791	403.85	1.9424
9	0.070385	20931	402.05	1.9208
15	0.070335	20970	406.27	1.9374
	Average			1.9337
	Standard Deviation:			0.0078
	Standard Deviation of the Mean:			0.0032
	Estimated Systematic Error: (0.5%)			0.0097

The variation of the full-energy-peak detection efficiency with gamma-ray energy was measured for the Ge(Li) detector using the ^{152}Eu source. The measurement was made with the source positioned far enough from the detector so that complicated geometry corrections could be avoided. The measurements were reproduced several times, and a smooth curve was fitted to the data. Then, both the ^{152}Eu and ^{137}Cs sources were used to measure absolute efficiencies for the Ge(Li) detector at a distant, reproducible, position. These data and the relative efficiency curve were used to determine the absolute efficiency for counting 412-keV gamma rays at the same position.

Next, several gold foils were irradiated in the ATSR to a sufficient level of activity to permit measurements to be made at the calibrated, distance position mentioned above. The gamma activities for these foils were determined in this fashion. Then, they were allowed to decay for several half lives and were subsequently counted in the close position which was used for the $^{6}Li(n,t)^{4}He$-to-$^{197}Au(n,\gamma)^{198}Au$ thermal cross section ratio experiment. These data, in conjunction with the known 412-keV gamma ray branch factor of 0.955 (± 0.1%)[13] were used to obtain an efficiency of 0.01935 (± 1.8%) for the Ge(Li) detector. This value is in remarkably good agreement with the value deduced from the $4\pi\beta$-γ measurements. Also, it should be noted that the measurements with the ^{152}Eu and ^{137}Cs sources yielded results which differed by only ~ 0.7%.

For the simultaneously irradiated lithium and gold foils, the neutron fluence had to be high enough to get reasonable tritium counting statistics. Therefore, the gold foils had much too high an activity to be immediately counted on the $4\pi\beta$-γ coincidence system with reasonable dead time losses. A wait time of about 3 weeks would have been required and this would have introduced an error of 0.6% due just to the uncertainty in the ^{198}Au half life. Since it was desired to determine the gold activity to the best accuracy possible, both the Ge(Li) detector and the $4\pi\beta$-γ coincidence counter were needed for these measurements.

III. CALCULATED $^{6}Li(n,t)^{4}He/^{197}Au(n,\gamma)^{198}Au$ ACTIVITY RATIO for THERMAL NEUTRONS

A. Thermal Neutron Flux Perturbation Due to An Absorbing Foil

The effect of an absorbing foil on a thermal neutron flux, both in the foil and in the surrounding medium, has been extensively treated by theoretical and experimental investigations. For an excellent review see Ref. 22. Suppose a purely absorbing foil is activated by an isotropic flux of monoenergetic neutrons. Following the notation of Hanna[23], the activity, A, per unit mass of a foil of radius R and thickness t relative to that of an infinitely thin foil, A_o, is

$$\frac{A}{A_o} = \frac{\alpha}{2\tau} \frac{1+\varepsilon}{1+g\alpha/2} \tag{1}$$

where τ is the foil thickiness in absorption mean free paths. The other quantities are defined below.

$$\tau \equiv \Sigma_a t = \frac{(m/A)}{AW} N_A \sigma_a \tag{2}$$

Here, (m/A), N_A, AW and σ_a are the foil mass per unit area, Avogadro's number, the atomic weight and the microscopic absorption cross section, respectively.

$$\alpha \equiv 1 - 2 E_3(\tau) \tag{3}$$

where $E_3(\tau) = \int_1^\infty x^{-3} e^{-\tau x} dx$

$$= \frac{1}{2} - \tau + \frac{\tau^2}{2}\left[\frac{3}{2} - \gamma - \ln \tau\right] \frac{\tau^3}{1\cdot 3!} - \frac{\tau^4}{2\cdot 4!} + \frac{\tau^5}{3\cdot 5!} \cdots$$

γ = Euler's constant = 0.57721566...

For tables and properties of the exponential integral $E_3(\tau)$ see Ref. 24. Hanna[23] has developed an approximate expression for ε, which is an edge effect correction for foils of finite radius.

$$\varepsilon = \frac{2\tau}{\alpha}\left(\frac{t}{\pi R}\right)\left[1 - \frac{\pi\tau}{6} - \Delta(2R\tau/t)\right] \tag{4}$$

Tabulated values of the function $\Delta(2R\tau/t)$ are given in Ref. 23.

The $\alpha/2\tau$ term in Eq. (1) is the correction for neutron self-shielding within the foil, while $[1 + g\alpha/2]^{-1}$ accounts for the neutron flux depression in the region surrounding the foil. In this expression, g is a function which depends only on the properties of the diffusing medium and on the foil radius. Again referring to Ref. 23,

$$g = g_s \, (g_v/g_s^{\infty}) \tag{5}$$

where

$$g_s = (3L/2\lambda)S(2R/L) - K(2R/\lambda,\gamma). \tag{6}$$

Here λ, L and γ are the total mean free path, the diffusion length, and the ratio of the total to the scattering mean free paths, respectively, of the diffusing medium. Also,

$$S(X) = \frac{4X}{3\pi} - \frac{X^2}{8} + \frac{4X^3}{45\pi} - \frac{X^4}{192} + \ldots \tag{7}$$

where $X = 2R/L$. Graphs of (g_v/g_s^{∞}) and $K(2R/\lambda,\gamma)$ are given by Ritchie and Eldridge[25]. To somewhat account for anisotropic scattering, λ may be replaced with λ_{tr}, the transport mean free path, in the equation for g_s[23]. For graphite, $\gamma \approx 1$ and [26]

$$K \approx (1/15) \, (2R/\lambda_{tr}) \text{ for } 2R<\lambda_{tr}. \tag{8}$$

Eq. (1) applies to the case of a pure absorber. For an infinite radius foil with a non-zero scattering cross section, the self shielding term may be written as [23].

$$\frac{A}{A_o} = \frac{\alpha(\tau_t)}{2\tau_t} + \frac{\tau_s}{2\tau_t} K(\tau_t),$$

provided the foil is thin enough so that second scattering events may be neglected. In this equation,

$$\tau_t = \Sigma_{tot} t \ , \quad \tau_s = \Sigma_s t$$

and

$$K(\tau_t) \approx 4.81\tau_t - 28.4\ \tau_t^2 + 74.7\ \tau_t^3 \ , \quad \tau_t < 0.15 \ .$$

To approximately account for scattering, Eq. (1) can be multiplied by the scattering correction factor (SCF),

$$SCF = \left[\frac{\alpha(\tau_t)}{2\tau_t} + \frac{\tau_s}{2\tau_t} K(\tau_t)\right] \Bigg/ \frac{\alpha}{2\tau} \ .$$

For the lithium and gold foils used in this calibration measurement,

$$SCF(Li) = 1.0018 \text{ and } SCF(Au) = 0.99995.$$

Therefore, scattering will be neglected from further consideration.

Eq. (1) is for monoenergetic neutrons and so must be modified for foils activated by thermal neutrons. For a 1/v purely absorbing foil in a Maxwellian spectrum in graphite, where g is nearly independent of neutron speed, Eq. (1) becomes [23]

$$\frac{A}{A_o} = \frac{\bar{\alpha}}{2\bar{\tau}} \ \frac{(1+\bar{\varepsilon})}{1+g\bar{\alpha}/2} \ . \tag{9}$$

$$\bar{\tau} = \int_o^\infty \tau(v) v^3 e^{-v^2/v_o^2} dv \Bigg/ \int_o^\infty v^3 e^{-v^2/v_o^2} dv$$

$$= \frac{\sqrt{\pi}}{2} \ \tau_o \ . \tag{10}$$

where τ_o is the value of τ at the most probable neutron speed v_o and where $\bar{\alpha}$ and $\bar{\varepsilon}$ are also Maxwellian-averaged values. Hanna[27] gives a series expansion for $\bar{\alpha}/2\bar{\tau}$, namely,

$$\frac{\bar{\alpha}}{2\bar{\tau}} = 1 - \frac{\tau_o}{\sqrt{\pi}}\left(\frac{3}{2} - \frac{3}{2}\gamma - \ln \tau_o\right) - \tau_o^2/3$$

$$+ 0.047016\ \tau_o^3\ (1.717 - \ln \tau_o) + 0.01111\ \tau_o^4 \qquad (11)$$

$$- 0.000784\ \tau_o^5\ (2.33 - \ln \tau_o) + \ldots$$

An approximate expression for $\bar{\varepsilon}^{23}$ is

$$\bar{\varepsilon} \approx \frac{2\bar{\tau}}{\bar{\alpha}}\left(\frac{t}{\pi R}\right)\left[1 - \frac{\sqrt{\pi}}{3}\tau_o - \Delta(2R\bar{\tau}/t)\right] . \qquad (12)$$

If the foil is irradiated in a cavity large enough so that a negligible number of neutrons passing through the foil are scattered back through the foil again, the flux is not depressed in the neighborhood of the foil. The only effect is that of neutron self-shielding within the foil. For this case Eq. (9) reduces to

$$\frac{A}{A_o} = \frac{\bar{\alpha}}{2\bar{\tau}}(1+\bar{\varepsilon}) \cdot \qquad (9a)$$

It was indicated in Section II.C that the disk on which the foils were mounted rotated in a void having a 4" x 13" cross section. Thus, about a 2 inch gap existed between the plane of the foils and the graphite on each side. In view of this geometry it is not entirely clear which equation, (9) or (9a), gives the better approximation. For this experiment the flux depression factor $[1+g\bar{\alpha}/2]^{-1}$ is very nearly equal to unity because the foils are thin and the diffusing medium is graphite and so Eqs. (9) and (9a) give nearly the same answer. A careful look at Eq. (9) shows that if the lithium and gold foils have the same effective thickness, τ, and equal radii, and if scattering effects within the foils are negligible, neutron flux perturbation effects cancel when activity ratios are determined. This condition was only approximately met in the present set of measurements.

How well Eq. (9) represents experimental foil activities as a function of thickness has been the subject of a number of studies. (See, for example, Refs. 22 and 23). Martinez[28] found that for a series of 1/2-in.-diameter indium foils ranging in thickness from 0.00002 in. to 0.020 in. irradiated by thermal neutrons in a graphite cube, Eq. (9) agreed with the experimental curve within the ± 2% experimental accuracy. For the thin lithium and gold foils used here the uncertainty in the application of Eq. (9) is expected to be less than 0.5%.

Finally, the activity per unit mass for an infinitely thin foil irradiated in a constant Maxwellian flux ϕ_{th} at temperature T = 293.6K for a time t_e is

$$A_o(t_e) = \frac{\sqrt{\pi}}{2} N_{act}\, \sigma_{act}(.0253eV)\, g\, \phi_{th}\, (1-e^{-\lambda t_e}) \qquad (13)$$

where

N_{act} = number of nuclei (^{6}Li or ^{197}Au) per gram of foil that can be activated.

σ_{act} = the 2200 m/sec activation cross section.

g = the Westcott g-Factor.

t_e = the time foil was exposed to the constant flux ϕ_{th} that began at time $t_e = 0$.

λ = the radioactive decay constant for the activated foil.

$A_o(t_e)$ = the foil activity per unit mass (dps/g) at time t_e.

B. Calculated Thermal Neutron ^{6}Li(n,t)^{4}He/^{197}Au(n,γ)^{198}Au Activity Ratio

From the equations given above the expected ^{6}Li(n,t)/^{197}Au(n,γ) thermal neutron activity ratio was calculated. The data used for this purpose are collected and shown in Table VIII. ENDF/B Version V[29] 2200 m/sec (.0253eV) cross sections were used with error estimates taken from Ref. 30. Table IX summarizes the numerical values of the various factors needed to evaluate A/A_o and the activity (per unit flux) A_o of an infinitely thin foil at the end of a t_e = 15.0 min irradiation. Finally, the ^{6}Li(n,t)/^{197}Au(n,γ) activity ratio was calculated to be

$$A\,[^{6}Li(n,t)^{4}He]\,/A\,[^{197}Au(n,\gamma)^{198}Au] = 2.7933 \times 10^{-3}\ (\pm\ 1.1\%).$$

The various factors contributing to the overall uncertainty in this calculated ratio are summarized in Table X.

Table VIII. Fundamental Data

Quantity		Value	Reference/Comments
Wt% Li in Foil		99.15	Table III
Wt% ^{6}Li		1.5512	Table III
Wt% Au in Foil		100%	Supplier Specif.
Wt% ^{197}Au		100%	
Foil Radius, R		0.9525 cm	R(Li) = R(Au)
Ave. Foil Mass/Area,	m/A(Li)	11.6868 mg/cm^2	
	m/A(Au)	24.6440 mg/cm^2	
Foil Density,	ρ(Li)	0.5383 g/cm^3	Ref. 31
	ρ(Au)	19.32	Ref. 22
Ave. Foil Thickness,	$\frac{m/A}{\rho}$, t(Li)	0.02171 cm	
	t(Au)	0.001276 cm	
Half Life,	$T_{1/2}$ (^{3}H)	12.33 ± 0.04 yr	Refs. 13, 14
	$T_{1/2}$ (^{198}Au)	2.697 ± 0.003 d	Ref. 13
Thermal Flux Exposure Time, t_e		15.0 min	
2200 m/sec Cross Sections (barn):			
^{6}Li	σ_t	936.64	ENDF/B-V
"	σ_s	0.71046	"
"	σ_γ	0.03850	"
"	σ_α	935.89 (± 0.43%)	"
^{7}Li	σ_t	1.086	"
"	σ_s	1.050	"
"	σ_γ	0.036	"
^{197}Au	σ_t	105.55	"
	σ_s	6.84	"
	σ_γ	98.71 (± 0.30%)	"
Westcott g-Factor:			
^{6}Li (n,t)^{4}He		1.00004	ENDF/B-IV
^{197}Au(n,γ)^{198}Au		1.00506	ENDF/B-III
Graphite Thermal Column:			
λ_{tr}		2.53 ± 0.03 cm	Ref. 26
L		54.2 ± 0.5 cm	Ref. 26

Table IX. Calculated $^{6}Li(n,t)^{4}He/^{197}Au(n,\gamma)^{198}Au$ Activity Ratio

Quantity	Calculated Values		Equation
	Li Foil	Au Foil	
$\tau_o \equiv \tau_{ao}$ (2200 m/sec value)	1.68778×10^{-2}	7.43757×10^{-3}	2
τ_{to} "	1.79187×10^{-2}	7.95295×10^{-3}	2
τ_{so} "	1.04092×10^{-3}	5.15378×10^{-4}	2
$\tau \equiv \tau_a$ "	1.49575×10^{-2}	6.59137×10^{-3}	10
$\alpha/2\tau$	0.95500	0.97675	11
$1+\epsilon$	1.00651	1.00043	12
g	0.42231	0.42231	6,7,8
$(1+g\alpha/2)^{-1}$	0.99400	0.99729	
A/A_o	0.95545	0.97452	9
$A_o(t_e)$ [per unit flux]	2.04766×10^{-6}	7.18705×10^{-4}	13
$A(^{3}H)/A(^{198}Au)$	2.79334×10^{-3} (± 1.1%)		

Table X. Error Estimate in Calculated $A(^{3}H)/A(^{198}Au)$ Activity Ratio

Quantity	Error %
N_{act} (^{6}Li)	0.8
σ_α (^{6}Li)	0.43
σ_γ (^{197}Au)	0.30
$T_{1/2}$ (^{3}H)	0.32
$T_{1/2}$ (^{198}Au)	0.11
A/Ao	0.4
Total*	1.1

*Added in quadrature.

IV. MEASURED $^{6}Li\ (n,t)^{4}He/^{197}Au(n,\gamma)^{198}Au$ ACTIVITY RATIO for THERMAL NEUTRONS

A. Tritium Activities

Lithium and gold foils were simultaneously irradiated in the ATSR graphite thermal column for 15 min at a power level of 5 kW on 4/10/80, as described in Section II.C. A second, but smaller, set of lithium and gold foils was irradiated on 4/17/80 at 10 kW for 15 min. Using the methods described earlier, tritium was extracted from each of the lithium samples, converted to tritiated water and counted by liquid scintillation methods. Each water sample was diluted with a carefully weighed amount of distilled water (~ 5 g). The diluted sample was divided into two equal amounts, each sealed in a 5 ml glass ampule. With the methods described in Section II.E, tritium activities were determined using two distinct liquid scintillation counting systems. For later reference, the Applied Physics Division counter will be referred to as the AP Counter, and the Chemical Engineering Division Tri-Carb System as the CE counter. Both counting systems were calibrated relative to the NBS standard, SRM 4926-C.[11]

Table XI gives the parameters needed to convert the measured activity in dps/g-H_2O to dps/g-Li foil. In this table m(F) is the lithium foil mass, m(C) the calculated water yield based on P, V and T measurements of the hydrogen initially present in the calibrated reservoir (Fig. 2), and m(E) the measured mass of collected water. Finally, m(D) is the mass of distilled water with which the sample was diluted. The last column in the table gives the multiplication factor for converting dps/g-H_2O to dps/g-Li foil.

The measured sample activities for both counting systems are summarized in Table XII. Errors shown in the table are random errors only and do not include estimates of systematic errors. Random errors were calculated on the

Table XI. Tritium Sample Parameters

ATSR Irrad.	Sample I.D.	Foil m(F), g	H_2O m(C), g	H_2O m(E), g	m(C)/m(E)	H_2O m(D), g	DF*	$\frac{[DF][m(C)]}{m(F)}$
4/10/80	Li-1	0.033136	5.76163	5.73035	1.00546	4.99543	1.87175	325.456
"	Li-2	0.033615	5.80376	5.75745	1.00804	5.01853	1.87166	323.149
"	Li-14	0.033266	5.81995	5.70625	1.01992	5.02577	1.88075	329.041
"	Li-16	0.033240	5.79453	5.75249	1.00731	5.11713	1.88955	329.394
"	Li-17	0.033420	5.78439	5.74048	1.00765	5.13082	1.89380	327.799
"	Li-30	0.033185	5.80152	5.76441	1.00644	5.03108	1.87278	327.406
4/17/80	Li-4	0.032855	5.90008	5.85829	1.00713	5.51586	1.94155	348.662
"	Li-9	0.030380	5.84448	5.80309	1.00713	5.49945	1.94768	374.693

*DF = dilution factor = [m(E) + m(D)]/m(E)

Table XII. Tritium Activities in Activated Lithium Foils (Random Errors Only)

ATSR Irrad.	Foil	dps/g-Foil (AP Counter)	dps/g-Foil (CE TRI-CARB)	Ave. dps/g-Foil
4/10/80	Li-1	5580 ± 47	5550 ± 34	5565 ± 29
"	Li-2	5636 ± 47	5530 ± 40	5583 ± 53
"	Li-14	5598 ± 35	5629 ± 34	5614 ± 24
"	Li-16	5642 ± 54	5693 ± 35	5668 ± 32
"	Li-17	5585 ± 53	5579 ± 34	5582 ± 31
"	Li-30	5625 ± 61	5588 ± 34	5606 ± 35
Weighted Mean:[a]		5608 ± 19	5597 ± 23	5605 ± 15
4/17/80	Li-4	11032 ± 98	11114 ± 63	11073 ± 58
"	Li-9	11005 ± 99	10210 ± 58	10608 ± 398
Weighted Mean:[a]		11019 ± 70	10625 ± 450	11063 ± 66

[a]The error in the weighted mean is taken as the larger value of $\sigma_{\bar{x}1}$ or $\sigma_{\bar{x}2}$ where $\sigma_{\bar{x}1} = \left[\Sigma_i\ \omega_i(\bar{x} - x_i)^2/(n-1)\Sigma_i\ \omega_i\right]^{1/2}$ and

$$\sigma_{\bar{x}2} = \left[\Sigma_i \left(\frac{\partial \bar{x}}{\partial x_i}\right)^2 \sigma_i^{\,2}\right]^{1/2} = \left[\Sigma_i\ \omega_i\right]^{1/2} .$$

$$\omega_i = 1/\sigma_i^{\,2} .$$

basis of pure counting statistics and for repeated counts for the same vial and for different vials containing the same sample. The larger of these errors is the one shown in Table XII.

This table shows that the AP and CE Counting Systems give tritium activities that are consistent with each other. The exception is foil Li-9 which is expected to have the same specific activity as foil Li-4. For the AP counter the measured activities for both foils are in good agreement. However, the CE TRI CARB system gives a Li-9 foil activity about 8% lower than that of foil Li-4. Since no explanation for this discrepancy has been uncovered, this highly suspect data point has not been rejected.

The known systematic errors for the lithium foil measurements are listed in Table XIII. Also listed is the weighted mean for the tritium activity per gram of foil at the end of each ATSR irradiation, together with the corresponding total (random plus systematic) error estimate.

Table XIII. Systematic Errors and Total Error in the Average Tritium Activity per Gram of Foil

Quantity	Systematic Error, %
NBS Calibration	0.63
Secondary Standard-Dilution Errors	0.04
Tritium Decay Correction	0.03
m(F)	0.03
m(C) - P, V, T measurements	0.12
m(E)	negl.
m(D)	negl.
TOTAL:	0.64

ATSR Irradiation	$\bar{A}(^3H)$ - dps/g Foil
4/10/80	5605 ± 39 (0.69%)
4/17/80	11063 ± 97 (0.88%)

B. Gold Activities

The gold foil activities were measured with a Ge(Li) gamma detector whose efficiency was determined by $4\pi\beta$-γ coincidence counting and with the use of calibrated gamma standards (see Section II.F). Activities were determined for single 1/2-mil thick gold foils and for sets of two 1/2-mil foils placed back-to-back in contact with each other. The results of these measurements are shown in Table XIV and Table XV, where activities have been adjusted to the time corresponding to the end of the ATSR irradiation.

The measured gold foil activities need to be corrected for the small contribution of the epithermal activation of the 4.9 eV resonance. Thus,

$$A = A_{th} + A_{epi}$$

$$A_{th} = A\left[1 - \frac{A_{epi}}{A_{Cd}}\ \frac{A_{Cd}}{A}\right] \equiv A[1 - F_{Cd}/CR]$$

where

A_{th} = activity due to thermal neutrons;

$CR = A/A_{Cd}$ = cadmium ratio, the activity of a bare foil to that of a cadmium covered foil;

$F_{Cd} = Aepi/A_{Cd}$ = correction factor for the absorption of epithermal neutrons by the cadmium covers.

The cadmium ratio for both single and double thickness 1/2-mil gold foils was measured at the same location in the graphite thermal column where the bare gold and lithium foils were irradiated. For these measurements cadmium covers 1.0 mm thick were used. From information given in Refs. 19 and 22, the F_{Cd} correction factor was determined. These quantities, together with the thermal neutron gold activities, are shown in Table XVI.

Because the $^{6}Li(n,t)^{4}He$ cross section does not have a low energy resonance, epithermal activation of the lithium foils is expected to be negligible. This can be shown in the following way. The cadmium ratio for the 1/v absorber may be written as (Ref. 22, p. 281):

Table XIV. Absolute Gold Foil Activities (Random Errors Only)

ATSR	Single Gold Foil			Double Gold Foils		
Irrad.	Foil	Mass(g)	dps/g, $\times 10^6$	Foil	Mass(g)	dps/g, $\times 10^6$
4/10/80	5	0.070325	2.0965 ± 0.0084	2	0.069865	2.0601 ± .0082
"	8	0.069920	2.1048 ± 0.0210	4	0.070050	2.0602 ± .0206
"	9	0.070385	2.0875 ± 0.0063	7	0.069885	2.0582 ± .0165
"	15	0.070335	2.1017 ± 0.0210	17	0.070075	2.0586 ± .0165
	Weighted Mean:[a]		2.0920 ± 0.0048			2.0596 ± .0064
4/17/80	10	0.070690	4.0304 ± 0.0252	11	0.068040	3.9799 ± 0.0159
				19	0.070780	3.9728 ± 0.0080
	Weighted Mean:[a]		4.0304 ± 0.0252			3.9742 ± 0.0071

[a]See note at bottom of Table XII.

Table XV. Systematic and Total Errors in the Average Gold Activity per Gram of Foil

Quantity	Systematic Error, %
Ge(Li) Detector Efficiency	0.53
^{198}Au Decay Correction	0.4
Gold Foil Masses	negl.
TOTAL:	0.67

ATSR Irradiation	A (^{198}Au) - dps/g, $\times 10^6$
4/10/80 Single Foil	2.0920 ± 0.0148 (0.71%)
4/17/80 Single Foil	4.0304 ± 0.0369 (0.92%)
4/10/80 Double Foil	2.0596 ± 0.0152 (0.74%)
4/17/80 Double Foil	3.9742 ± 0.0276 (0.69%)

Table XVI. Thermal Neutron Gold Foil Activities

ATSR Irrad.	Thickness(μ) $t = \frac{m/A}{\rho}$	F_{Cd}	CR	$[1 - F_{Cd}/CR]$	A_{th} dps/g, $\times 10^6$
4/10/80	12.8	1.085	209 ± 2	0.9948	2.0811 (±0.71%)
	25.4	1.110	271 ± 3	0.9959	2.0512 (±0.74%)
4/17/80	12.8	1.085	209 ± 2	0.9948	4.0095 (±0.92%)
	25.2	1.110	271 ± 3	0.9959	3.9579 (±0.69%)

$$CR = \frac{1}{r} \frac{\sqrt{\pi}}{4} [E_{Cd}/kT]^{1/2}$$

where E_{Cd} is the cadmium cut-off energy (~ 0.67 eV for 1 mm cadmium covers) and kT is the neutron energy corresponding to the most probable speed in a Maxwellian flux (i.e. 0.02533 eV at T = 293.6 K). In a soft spectrum, r is approximately equal to the ratio of the epithermal-to-thermal flux. One can evaluate r from a measurement of the cadmium ratio for a thin gold foil for which the resonance integral is known. Again from Ref. 22, p. 278, for a thin foil:

$$CR - F_{Cd} = \frac{1}{r} \frac{\sqrt{\pi}}{2} g(293.6\ K)\ \sigma_{act}(2200\ m/sec)/RI$$

where $RI = \int_{E_{Cd}}^{\infty} \sigma_{act}(E)dE/E$ = resonance integral

g = Westcott g-factor at T=293.6 K.

For a 1/2-mil gold foil,

$CR = 209$

$F_{Cd} = 1.085$

$g = 1.00506$ ENDF/B-III

$\sigma_{act} = 98.71$ b ENDF/B-V[29]

$RI = 1562$ b ENDF/B-V[32]

From this data and the above equations the cadmium ratio for the lithium foils was estimated to be

$$CR(Li) \approx 8.4 \times 10^3.$$

Hence,

$$\frac{A_{th}}{A} = [1 - F_{Cd}\ (Li)/CR] = 1 - 2.8/8.4 \times 10^3 = 0.9997;$$

therefore, no epithermal activation correction was applied to the lithium foil activities.

C. Measured Thermal Neutron $^6Li(n,t)^4He/^{197}Au(n,\gamma)^{198}Au$ Activity Ratio

From the data in Tables XIII and XVI the measured thermal neutron activity ratio $^6Li(n,t)/^{197}Au(n,\gamma)$, AR(E), can be evaluated. The result for the 1/2-mil gold foils is shown in Table XVII. Finally, the measured and calculated activity ratios, AR(E) and AR(C), are compared in Table XVIII.

Table XVII. Measured Thermal Neutron $^6Li(n,t)^4He/^{197}Au(n,\gamma)^{198}Au$ Activity Ratio, AR(E)

ATSR Irrad.	AR(E)	Random Error, %	Systematic Error, %	Total Error, %
4/10/80	2.693×10^{-3}	0.35	0.93	0.99
4/17/80	2.759×10^{-3}	0.86	0.93	1.27
Weighted Mean	2.702×10^{-3}	0.84	0.93	1.25

Table XVIII. Comparison of the Calculcated (C) and Measured (E) $^{6}Li(n,t)^{4}He/^{197}Au(n,\gamma)^{198}Au$ Thermal Neutron Activity Ratio

AR(C)	AR(E)	C/E
2.793×10^{-3} (± 1.1%)	2.702×10^{-3} (± 1.3%)	1.033 ± 0.018

V. CONCLUSION

The system used to extract and count tritium from neutron-irradiated lithium metal samples has been calibrated by a thermal neutron activation technique. Thin lithium and gold foils were simultaneously activated in the graphite thermal column of the ASTR reactor such that the neutron fluence was the same for each foil. Using previously developed methods, tritium was extracted from each lithium sample, converted to tritiated water, and counted by standard liquid scintillation methods on two different systems. Gold foil activities were measured with a Ge(Li) detector calibrated by $4\pi\beta$-γ coincidence counting.

The measured $^{6}Li(n,t)^{4}He/^{197}Au(n,\gamma)^{198}Au$ thermal neutron activity ratio was found to be $(2.702 \pm 0.034)\times10^{-3}$. Using the well-known thermal neutron cross sections and making flux perturbation corrections, the calculated ratio was found to be $(2.793 \pm 0.031)\times10^{-3}$. Therefore, the calculated-to-measured ratio is C/E = 1.033 ± 0.018.

Two conclusions follow from this result:

1) In the Bretscher/Farrar experiment (see Appendix) the helium concentration was found to be 9% larger than the tritium concentration for neutron-activated natural lithium samples. This 9% discrepancy cannot be the result of systematic errors associated with the tritium extraction and counting techniques, as the above C/E ratio demonstrates.

2) On the basis of this calibration, we do not recommend adjusting any of the previously measured $^{6}Li(n,t)\alpha$ reaction rates in the various ZPR fast critical experiments nor the recently determined $^{7}Li(n,n't)\alpha$ cross sections for systematic tritium losses of unknown origin. Although the error assigned to the C/E ratio does not overlap unity, this error is the 1 σ value. Thus, within the 95% confidence level the C/E ratio is indeed unity. Furthermore, most of the error assigned to the C/E ratio arises from uncertainties in the $^{6}Li(n,\alpha)$ and $^{197}Au(n,\gamma)$ thermal cross sections, the ^{3}H and ^{198}Au half lives, the calibration of the NBS tritiated water standard, and the ^{6}Li content of the foil material. Except for the ^{6}Li concentration, errors assigned to these quantities are literature-recommended values and, at least in some cases, may be unrealistically small.

ACKNOWLEDGEMENTS

Many individuals have contributed in important ways to these measurements. E. F. Lewandowski designed and fabricated the extrusion die for making thin lithium foils and developed the process of cladding the foils in aluminum. The lithium foils were extruded, punched, weighed, and clad by R. R. Hopf. R. Rutkowski did most of the tritium extractions. Liquid scintillation counting using the TRI-CARB equipment was done by D. L. Bowers while W. P. Poenitz provided valuable guidance for the $4\pi\beta$-γ coincidence counting of the gold foils. The lithium mass spectrum was measured by E. L. Callis (ANL) and J. R. Walton (ORNL). ATSR irradiations were performed under the supervision of R. J. Armani. The contributions from each of these individuals are most gratefully acknowledged.

APPENDIX: THE BRETSCHER/FARRAR COMPARISON

This experiment was designed to test the tritium extraction and counting procedures used at ANL to measure absolute neutron absorption rates in lithium metal samples irradiated in the ZPR fast critical assemblies. For tritons produced in the $^{6}Li(n,\alpha)^{3}H$ reaction, an equal number of alpha particles are generated. This experiment consisted of measuring both the tritium and helium produced in natural lithium metal samples exposed to the same neutron fluence. The tritium extraction and counting was done at ANL. Dr. Harry Farrar from Rockwell International (RI), Canoga Park, California, measured the helium accumulation in the samples using very specialized mass spectrometer techniques.

Samples were prepared in a glove box containing high purity argon (99.999%). To remove dissolved helium, the natural lithium metal was melted in the glove box and pure argon was allowed to bubble through the liquid for one hour. Following this operation, the molten lithium was poured into an extrusion die and then maintained at 260°C in vacuum for 21 hours. After cooling to room temperature, lithium wire 1.8 mm diameter was extruded, cut into 18 mm lengths, weighed, and sealed by cold welding in aluminum (Type 1100) capsules 20 mm long and 2.4 mm o.d. All these operations were performed in the high purity argon-filled glove box.

Fifteen of these samples were irradiated on a rotating disk located in the graphite thermal column of the ATSR reactor so that each sample was exposed to the same neutron fluence. Eight of these samples were analyzed at ANL for tritium content using the same methods described in Sections II.D and II.E of this report.

The remaining samples, including unirradiated ones, were sent to RI for helium analyses. In its simplist form, the helium analysis consists of vaporizing the lithium capsule, spiking the sample gas with a calibrated

quantity of ^3He, and using a mass spectrometer to measure the $^4He/^3He$ ratio. It was observed that the presence of argon in the samples caused the release of helium adsorbed from previously-measured larger samples due to the inert gas bombarding the system walls. This "helium memory effect" problem was overcome by using a new furnace and a liquid-nitrogen-cooled charcoal trap getter which were reserved for use only with small helium samples. A correction of ~ 0.2% had to be applied for ^4He released from unirradiated lithium samples.

The results of the measurements of the tritium and helium concentrations are summarized in Table A-I. Details of the helium measurements have been published in a number of Atomics International reports (see Refs. 33 and 34). This table shows the measured helium concentration is about 9% larger than that determined for tritium. A number of investigations were performed to try to resolve this discrepancy.

^3He builds up in the irradiated samples as a function of time because of the beta decay of tritium. For this reason, several of the samples analyzed by H. Farrar were not initially spiked with ^3He so that both the ^3He and ^4He content in the samples could be measured, though perhaps with somewhat less precision than that obtained by the spiking technique. Assuming ^4He and ^3H are produced in equal quantities during the irradiation, one can easily calculate, from the half life of tritium, how the $^4He/^3He$ ratio decreases as a function of time. Farrar's measured and calculated $^4He/^3He$ ratios[34] are compared in Table A-II, where a tritium half life of 12.33 yrs was used. The first two samples in this table were analyzed within 2 weeks of the irradiation and the last two about 440 days later. For the last two samples the measured and calculated ratios agree within the estimated ± 1% (1σ) uncertainty of the measurement. These results indicate that:

Table A-I. ^{3}H and ^{4}He Production from the $^{6}Li(n,\alpha)^{3}H$ Reaction

Sample	Li Mass mg	^{3}H Concentration (10^{15} atoms/g Li)	^{4}He Concentration[a] (10^{15} atoms/g Li)
10	22.700	1.329	
11	22.895		1.425
12	22.610	1.317	
13	22.850		1.437
14	22.360	1.307	
15	22.765		1.477
16	22.740	1.329	
17	22.770		1.464
18	22.715	1.311	
19	22.690		1.452[c]
20	22.650	1.323	
21	22.640		1.447[c]
22	22.800	1.362[b]	
23	22.640		1.469
24	22.800	1.360[b]	
Weighted Mean:		1.330 ± 0.015[d]	1.455 ± 0.004

[a]See Ref. 34.
[b]Analyzed ~ 261 days after initial set.
[c]Analyzed ~ 440 days after initial set.
[d]Combined systematic error (0.95%) and random error (0.55%). Systematic error arises from NBS calibration and uncertainty in tritium half life.

Table A-II. Helium Generation in Irradiated Lithium Samples[a]

Sample	Lithium Mass mg	$^{4}He/^{3}He$ Ratio Measured	Calculated
11	22.895	686	660
15	22.765	376	387
19	22.690	14.79	14.66
21	22.640	14.55	14.60

[a]See Ref. 34.

1) No measurable amount of tritium leaked from the sample before analysis.

2) No significant amount of ^4He was produced in the sample from (n,α) reactions due to sample impurities such as boron.

3) Systematic errors associated with ^3He and ^4He measurements must be small.

The absolute calibration of the high sensitivity mass spectrometer used for these helium analyses was checked by measuring the helium concentration in the earth's atmosphere.[34] The measured results agreed within 1% of the currently accepted value.[35]

One more test is underway at Rockwell International. Aliquots of tritiated water from the ANL extractions, along with a sample of the NBS tritiated water standard, have been supplied to RI for special helium measurements. After pumping out all helium from these water samples, known quantities of water will be sealed in vials of Corning Type 1720 glass which is very impervious to helium. After a known period of time the samples will be analyzed for ^3He resulting from the beta decay of tritium, following a technique first used by W. B. Clarke, W. J. Jenkins and Z. Top.[37] Results from these measurements will allow a direct comparison of tritium activities measured at ANL with those found from the ^3He determinations, as well as an independent calibration of the NBS tritiated water standard.

The ANL tritium extraction and liquid scintillation counting procedures also have been carefully re-examined. Tritiated water samples were prepared from both the old and the new[36] NBS standards. The ratio of measured activities was found to be in excellent agreement with that calculated from

the calibration data. For the measurements reported in Table I the old NBS standard had been used. Within the accuracy of the measurements (~ 0.5%), light-quenching effects in water produced by the extraction process were the same as in distilled water used to prepare secondary tritium standards. Tritium activities were measured as a function of the time that the hydrogen-tritium mixture remained in the lithium oven before being allowed to flow over the hot CuO bed (see Fig. 2 of this report). For times of 45 (normal operation) 90, and 135 min, no observable change in the tritiated water activities was observed. Measured tritium activities were also found to be independent over a wide range of hydrogen flow conditions. Normally hydrogen flows continuously from the lithium oven, through a metering valve, and across the CuO until all of the initial hydrogen in the reservoir has been used (see Fig. 2). In some measurements, however, the initial hydrogen-tritium mixture was pumped through the CuO oven and converted to ice in liquid nitrogen traps before additional hydrogen from the reservoir was flushed through the system. The same activities were measured for the discontinuous as for the continuous hydrogen flow conditions.

The origin of the ~ 9% discrepancy between the Rockwell International helium measurements and the ANL tritium measurements remains a mystery. From the measurements described above, there does not appear to be a bias in the mass spectrometer helium measurement method. At the same time the $^{6}Li(n,\alpha)^{3}H/^{197}Au(n,\gamma)^{198}Au$ thermal calibration measurements given in this report indicate that the 9% discrepancy cannot be attributed to systematic errors associated with the tritium extraction and counting procedures. Without additional ANL/RI comparisons, it appears very unlikely that this matter will be fully resolved.

REFERENCES

1. M. M. Bretscher, "Li-6 as a Reference Absorber for Capture-to-Fission Ratio Measurements in Zero Power Fast Critical Assemblies," Reactor Physics Division Annual Report, July 1, 1967 to June 30, 1968, ANL-7410, pp. 178-182, Argonne National Laboratory (1969).

2. M. M. Bretscher and W. C. Redman, "Low Flux Measurements of ^{239}Pu and ^{235}U Capture-to-Fission Ratios in a Fast Reactor Spectrum," Nucl. Sci. Eng. 39, 368 (1970).

3. M. M. Bretscher, J. M. Gasidlo, and W. C. Redman, "A Comparison of Measured and Calculated ^{239}Pu, ^{235}U and ^{238}U Integral Alpha Values in a Soft Spectrum Fast Critical Assembly," Nucl. Sci. Eng. 45, 87 (1971).

4. M. M. Bretscher, J. M. Gasidlo and D. W. Maddison, "^{240}Pu Absorption-to-Fission Ratio Measurements in a Fast Reactor Spectrum," Trans. Am. Nucl. Soc., 21, 456 (1975).

5. M. M. Bretscher and J. A. Morman, "Integral Alpha and Point Conversion Ratio Measurements in Advanced Fuels Critical Assemblies," Trans. Am. Nucl. Soc., 28, 783 (June 1978).

6. W.C. Redman and M. M. Bretscher, "Experimental Determination of the Perturbation Denominator in Fast Critical Assemblies," Nucl. Sci. Eng. 44, 450 (1971).

7. S. G. Carpenter, et al., "Measurement and Analysis of the Breeding Ratio in ZPPR Assembly 4, Phase 1", Trans. Am. Nucl. Soc., 22, 693 (1975).

8. D. L. Smith, M. M. Bretscher and J. W. Meadows, "Measurement of the Cross Section for the $^{7}Li(n,n't)\alpha$ Reaction in the Energy Range 7-9 Mev," to be submitted to Nucl. Sci. and Eng. for publication.

9. F. Brown, et al. "The Cross Section of the $^{7}Li(n,t)$ Reaction for Neutron Energies Between 3.5 and 15 Mev," J. Nucl. Energy 17, 137 (1963).

10. P. S. Flint, "The Diffusion of Hydrogen Through Materials of Construction", KAPL-659 (1961); D. Randall and O. N. Salmon, "The Permeability of Type 347 Stainless Steel to Hydrogen and Tritium," KAPL-904 (1953); N. J. Hawkins, Solubility of Hydrogen Isotopes in Nickel and Type 347 Stainless Steel," KAPL-868 (1953); R.R. Heinrich, C. E. Johnson and C. E. Crouthamel, "Hydrogen Permeation Studies," J. Electrochem. Soc. 112, 1067 (1965).

11. Tritiated Water: SRM 4926-C, U.S. National Bureau of Standards, Office of Standard Reference Materials, Room B-311, Chemistry Building, Washington, D.C. 20234, U.S.A.

12. James Gray, Argonne National Laboratory, private communication (6/80).

13. Table of the Isotopes, 7th Edition, Ed. C. Michael Lederer and Virginia S. Shirley, John Wiley and Sons, Inc., New York (1978).

14. R. Sher, "Half Lives of ^{3}H and ^{238}Pu", BNL-50233 (1970).

15. A. DeVolpi and M. M. Bretscher, "Development of an Improved Tritium Counting Facility." Applied Phsyics Division Annual Report, July 1, 1969 to June 30, 1970, ANL-7710, p. 296, Argonne National Laboratory (1971).

16. J. E. Noakes, M. P. Neary and J. D. Spaulding, "Tritium Measurements with New Liquid Scintillation Counter," Nucl. Instr. and Meth. 109, 177 (1973).

17. A. A. Moghissi, et al., "Low-Level Counting by Liquid Scintillation-Part I. Tritium Measurement in Homogeneous Systems," Int. J. Appl. Rad. Isotopes 20, 145 (1969). See p. 150

18. Model 2660 Packard Tri-Carb Liquid Scintillation Counter: Packard Instrument Co., Inc., 2200 Warrenville Road, Downers Grove, Ill. 60515.

19. Wolfgang Poenitz, "Determination of Absolute Thermal Neutron Flux by Gold Foils," Institut fur Agnewandte Kernphysik, Kernforschungszentrum Karlsruhe, KFK 180 (April 1963).

20. ^{137}Cs Source: SRM 4207-187, U.S. National Bureau of Standards, Office of Standard Reference Materials, Washington, D.C. 20234, U.S.A.

21. ^{152}Eu Source: No. 5243, Laboratoire de Metrologie des Rayonnements Ionisants, Bureau National de Metrologie, Saclay, BP No. 2-91190 Gif-sur-Yvette, France.

22. K. H. Beckurts and K. Wirtz, "Neutron Physics," Springer-Verlag, New York Inc. (1964), Chap. 11.

23. G. C. Hanna, "The Neutron Flux Perturbation Due to an Absorbing Foil; A Comparison of Theories and Experiments," Nucl. Sci. Eng. 15, 325 (1963).

24. "Handbook of Mathematical Functions with Formulas, Graphs, and Mathematical Tables", Ed. M. Abramowitz and I. A. Stegun, National Bureau of Standards Applied Mathematics Series 55, U.S. Government Printing Office, Washington, D.C. (1965).

25. R. H. Ritchie and H. B. Eldrige, "Thermal Neutron Flux Depression by Absorbing Foil," Nucl. Sci. Eng. 8, 300 (1960).

26. Reactor Physics Constants, ANL-5800 (1963).

27. G. C. Hanna, "The Depression of Thermal Neutron Flux and Density by Absorbing Foils," Nucl. Sci. Eng. 11, 338 (1961).

28. J. S. Martinez, "Neutron Self-Sheilding in One-Dimensional Absorbers," UCRL-6526 (1961).

29. R. Kinsey, "ENDF/B Summary Documentation," BNL-NCS-17541 (ENDF-201) 3rd Editon (ENDF/B-V) UC-80 (July 1979).

30. S. F. Mughabghab and D. I. Garber, "Neutron Cross Sections - Volume I, Resonance Parameters," BNL 325 3rd Edition (June 1973).

31. J. W. Mausteller, F. Tepper and S. J. Rodgers, "Alkali Metal Handling and System Operating Techniques", Gordon and Breach, Science Publishers, New York (1967). Note: The density of natural lithium (0.534 g/cm^3) was adjusted to that of the isotopic composition shown in Table VII.

32. N. E. Holden, "$^{197}Au(n,\gamma)^{198}Au$ Thermal Neutron Cross Section", ENDF-300 Standard Reference and Other Important Nuclear Data by the Cross Section Evaluation Working Group BNL-NCS-51123 UC-34c (December 1979).

33. H. Farrar IV, J. G. Bradley, and B. M. Oliver, "Technical Progress Reports - Fast Reactor Dosimetry for Period June-December 1977," AI-DOE-13209, Atomics International, March 1978.

34. B. M. Oliver, J. G. Bradley, and Harry Farrar IV, "Technical Progress Report - Fast Reactor Fluence Dosimetry for Period October 1978 - March 1979," ESG-DOE-13310, Rockwell International, January 1980.

35. E. Gluckauf, "A Micro-Analysis of the Helium and Neon Contents of Air," Proc. Roy. Soc., A185, 98 (1946).

36. Tritiated Water: SRM 4926-C, U.S. National Bureau of Standards, Office of Standard Reference Materials, Room B-311, Chemistry Building, Washington, D.C. 20234. Specific activity is 3.406×10^3 × 0.63% dps/g as of 9/3/78. The activity of the old standard (SRM-4926) was 8.780×10^3 ± 0.6% as of 9/31/61.

37. W. B. Clark, W. J. Jenkins and Z. Top, "Determination of Tritium by Mass Spectrometric Measurement of ^3He," Int. J. Appl. Rad. Isotopes 27, 515 (1976).